

Extreme Astrophysics

Raghavan Gopalan (14994593)

University of Amsterdam 2023

Introduction

In this project, we study the Low- Mass X-Ray Binary GS2023+338 (V404 Cygni) in the hard-state. Some general information about the source is provided below:

- Mass of the Black Hole: $9M_{\odot}$ (Koljonen, K. I. I. & Tomsick, J. A. (2020))
- Distance from Earth: 2.39 kpc (Koljonen, K. I. I. & Tomsick, J. A. (2020))
- Companion Star mass: $1.5M_{\odot}$ (Khargharia et al. (2010))
- Companion Star spectral type: K3 III (Khargharia et al. (2010))
- Orbital period : 6.473 days (Bartolomeo Koninckx, L. et al. (2023))
- Inclination: 60° (Koljonen, K. I. I. & Tomsick, J. A. (2020))

V404 Cyg undergoes infrequent outbursts, with only 2 recorded in the last 50 years (1989 and 2015). It generally remains in a quiescent state during other periods, with a much lower accretion rate and luminosity in this phase. However, being one of the closest X-ray binaries known to us, it has been studied extensively. The quiescent state has been shown to have a significant correlation with the hard state for V404 Cygni (Bernardini et al. (2016)), therefore we will be modelling V404 Cygni assuming common hard-state geometry and parameters, i.e. a thermal accretion disk and a spherical corona.

1 Methodology

Our model assumes the corona to be the equivalent of the base of a jet observed in black holes. We assume a constant magnetic field throughout the corona and assume that equipartition is valid ($U_e = U_b$). In order to simulate a spectrum, we first created the spectra for the Cyclo-synchrotron emission from the corona and the black body emission from the disk. We then used a Monte Carlo code to simulate inverse Compton scattering of these two components. Finally,

We assumed that corona was spherical and that it had a radius of $10 r_g$. We took the range of lorentz factors of the particles in the corona to be from $\gamma = 1$ to $\gamma = 100$.

1.1 Self-Absorbed Cyclo-Synchrotron

This is the emission produced by the corona due to electrons (non- relativistic and relativistic) travelling through the corona's magnetic field. Here, we assume a constant magnetic field of 33G as given by Dallilar et al. (2017) and an electron number density of 10^{15} cm^{-3} . It has two components:

1. Cyclotron- For cyclotron radiation, we assume the electrons are purely thermal and follow a Maxwell-Juttner distribution in momentum space given by equation (6) in Lucchini et al. (2022) with the temperature of the corona estimated as 10^8 K (Motta et al. (2017)). The lorentz factors of the electrons were taken to be in the range [1.1,2]. The emissivity per frequency for each lorentz factor was calculated using equation (16), then integrated over the range of lorentz factors, taking into the Maxwell Juttner distribution, as prescribed in equation (17) of Lucchini et al. (2022). 2. Synchrotron- For synchrotron radiation, we assume the particles follow a power law distribution (our best fit was found to be for a power law index of 3.5). The emissivity is then calculated using equation 6.36 of Ryb (1985) . The normalization constant

C is found using equipartition considerations, where we have arrived at the following parameters after multiple fits:

1. L_j : Luminosity of the jet (corona in our case) = $10^{-4} L_{edd}$
2. v : Bulk velocity of the material flowing through the corona = $0.5 \times c$, where c is the speed of light
3. A : Area of the corona, this is corresponding to the assumption we have made throughout that the corona is a sphere of radius $10 r_g$.

After obtaining the emissivity, we correct for extinction within the corona using the absorption coefficient equation (6.53) given in Ryb (1985). We then obtain the optical depth by integrating over the diameter of the corona, and arrive at a specific intensity for self-absorbed cyclo-synchrotron radiation. Following this, we integrate over solid angles and account for geometric dilution to obtain a flux density observed at Earth.

Self-absorbed cyclotron and synchrotron radiation can be observed at their respective characteristic gyrofrequencies, given by:

$$\nu_{cyclotron} = \gamma^2 \frac{eB}{2\pi mc}$$

$$\nu_{synchrotron} = \gamma^2 \frac{3eB}{2mc}$$

where γ are the respective electron lorentz factors.

1.2 Inverse Compton Scattering

In order to simulate Inverse Compton scattering off of the Corona, we modified a Monte Carlo code provided to us (Sebastian Heinz (2023)). We assumed a Maxwell-Juttner distribution of velocities in the corona; we sampled from this distribution at a temperature of 10^8 K and implemented this sampling function into the Monte Carlo code. A constant optical depth was assumed in the corona (independent of frequency).

The Monte Carlo code samples a photon from the photon field and an electron distribution randomly and scatters them relativistically; this is done by going into the frame of the electron, performing the calculations required for thomson scattering, and going back into the lab frame after the scattering. The direction and of the velocities and scattering are randomized and assumed to be isotropic (in the rest frame of the electron). This process is repeated until the photon escapes the corona and then repeated for n number of photons in order to obtain a distribution of energies of photons leaving the corona.

For the black body emission of the disc, we assumed a Planck function at a temperature of 10^7 K and sampled off of this for the Monte Carlo code. (JAMES B. DOVE (1997) find a high black body temperature consistent with their model for V404 Cygni).

For the SSC component, we converted our intensity spectrum obtained in 1.1 into a photon number distribution and subsequently sampled from that for the Monte Carlo code.

We then converted our final output, in the form of energies of photons exiting the Corona (for both SSC and IC of the BB), into a flux spectrum.

2 Results

Sampling from the Maxwell-Juttner distribution gave us an energy distribution as shown in figure 1. This sampling function is the one implemented in the Monte Carlo code in order to obtain a random velocity of an electron in the corona.

The combined input photon field - that is, the Cyclo-synchrotron component and the black body component - is shown in fig 2. This plot shows the intensity values before they have been Compton scattered by the Corona. The two components of this plot are sampled from while running the Monte Carlo simulations.

The final flux spectra, shown in fig 3, shows the various components that were modelled along with the data taken from Motta et al. (2017) for the X-ray region and Bernardini et al. (2016) for the radio regime. We varied our parameters such that our frequencies lie in appropriately matching regions of the plot while giving a lower priority to getting the value of the flux exactly right.

Lastly, we have the combined flux, shown in fig 4, with overlapping components summed up and the unique components being displayed along with data points. However, we feel that figure 3 is more informative to the reader interested in understanding the different contributing emission processes. This figure can be rather confusing as there are still 2 sets of model points in the 10^{12} Hz range.

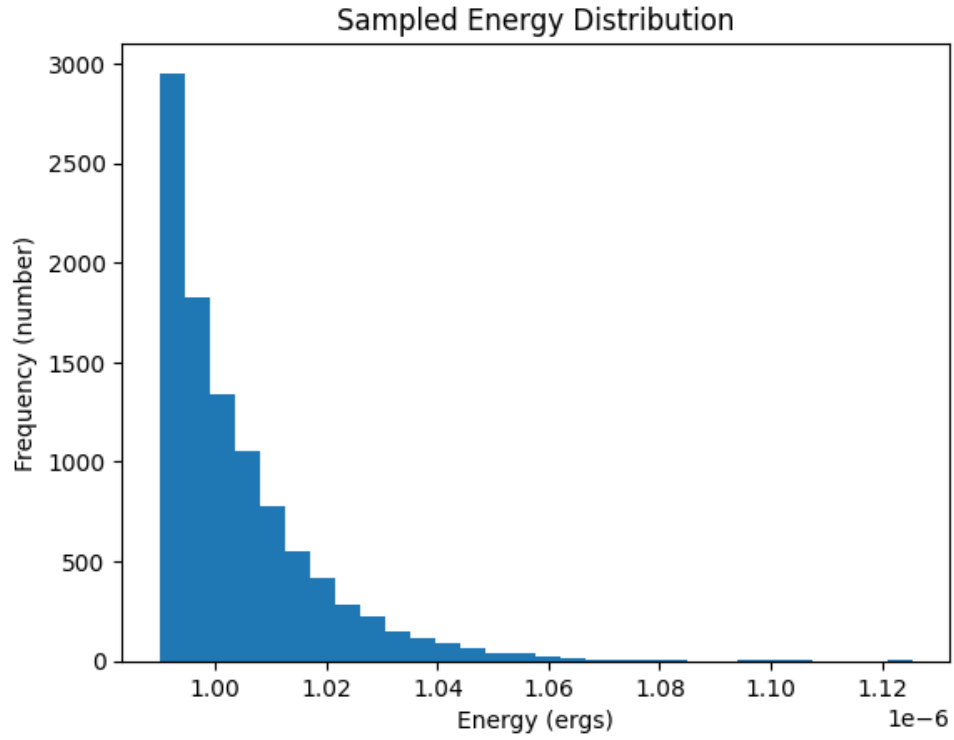


Figure 1: The sampled energy distribution of electrons in the corona at a temperature of 10^8 Kelvin.

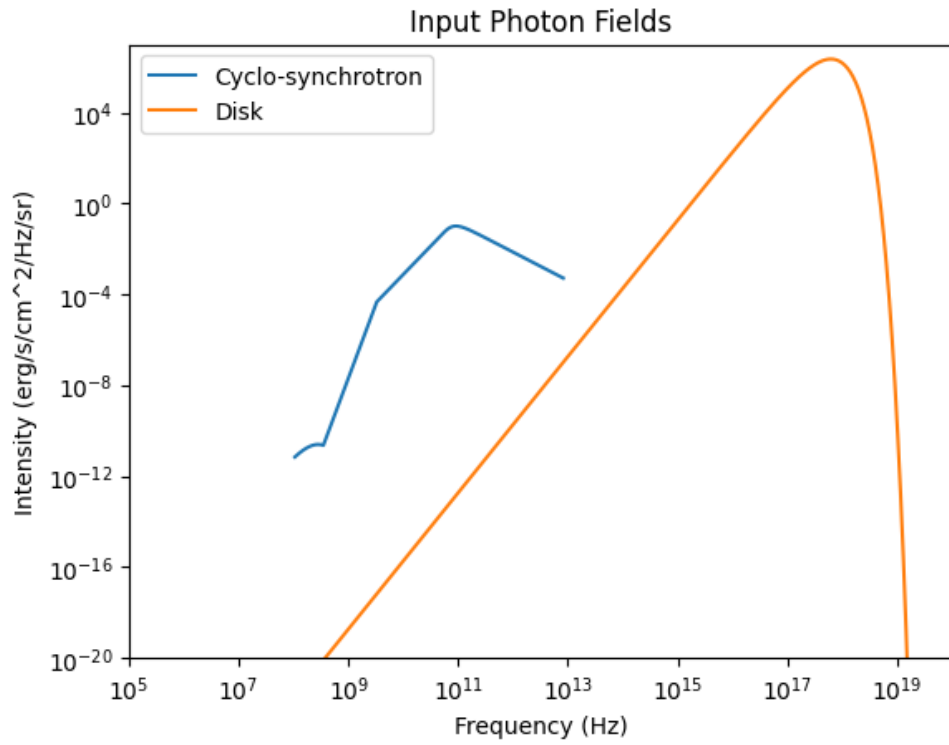


Figure 2: Input photon field (black body and Cyclo-synchrotron) for the Monte Carlo simulation

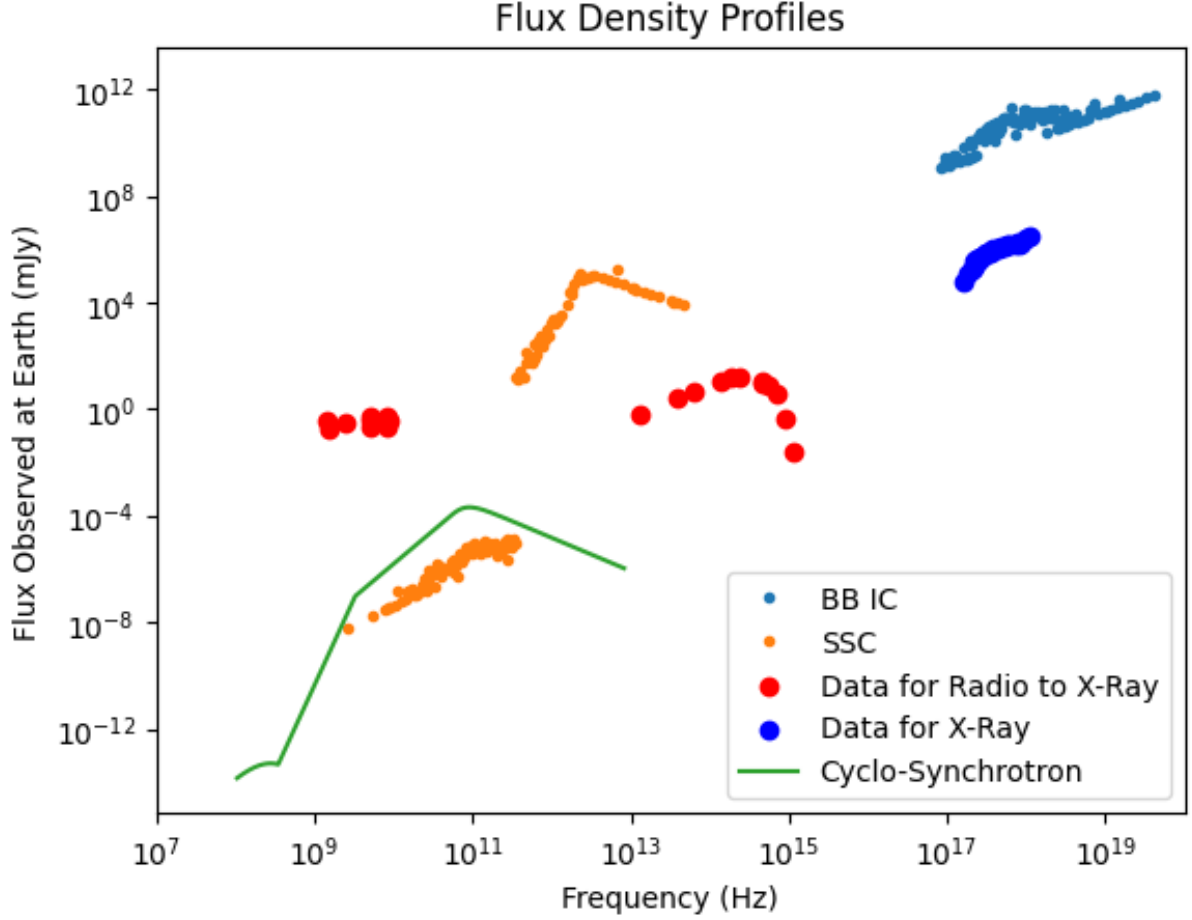


Figure 3: Modelled flux spectra (green, orange and cyan) along with data (red and blue). The straight line indicates the Cyclo-synchrotron spectrum before IC scattering. The smaller orange and cyan dots indicate the results after IC scattering for the Cyclo-synchrotron and disk components. The larger red and blue dots indicate data taken for the radio and x-ray regime respectively

3 Verifications and Sources of Error

Overall, we've modelled a cyclosynchrotron self absorption, a Synchrotron self compton and an Inverse Compton component from the accretion disk. We have made many assumptions along the way that have led to some under or over-estimations. Below, I will attempt to explain why some parts of our outputs are correct or why they deviate from literature or observations, and potential fixes.

1. Magnetic field strength calculation from Longair fitting formula:

The fitting formula is given by $\nu_{ssa} = (100 \text{ MHz}) B_{mG}^{4/3} R_{kpc}^{1/3}$

For $\nu_{ssa} = 10^{11} \text{ Hz}$, $R_{kpc} = 10 r_g / (3 \times 10^{21})$, we obtain $B \sim 700 \text{ G}$.

This is about 1 order of magnitude off the observed value of 33G, suggesting that our value of ν_{ssa} is likely close to correct. This is also supported by our synchrotron spectrum peak being slightly to the right of the observed radio data. I will discuss possible reasons for this in the next point.

2. Equipartition magnetic field and plasma beta calculations:

The output of the calc_B function in the modelling code is the magnetic field strength of the corona assuming equipartition division of magnetic field energy density and electron energy density. This is a field strength of 207252 G and can also be visualized using an order of magnetic calculation:

$$U_B = B^2 / (8\pi)$$

$$U_{tot} = 2 U_B$$

$$U_{tot} = L_j / (4\pi R^2 v)$$

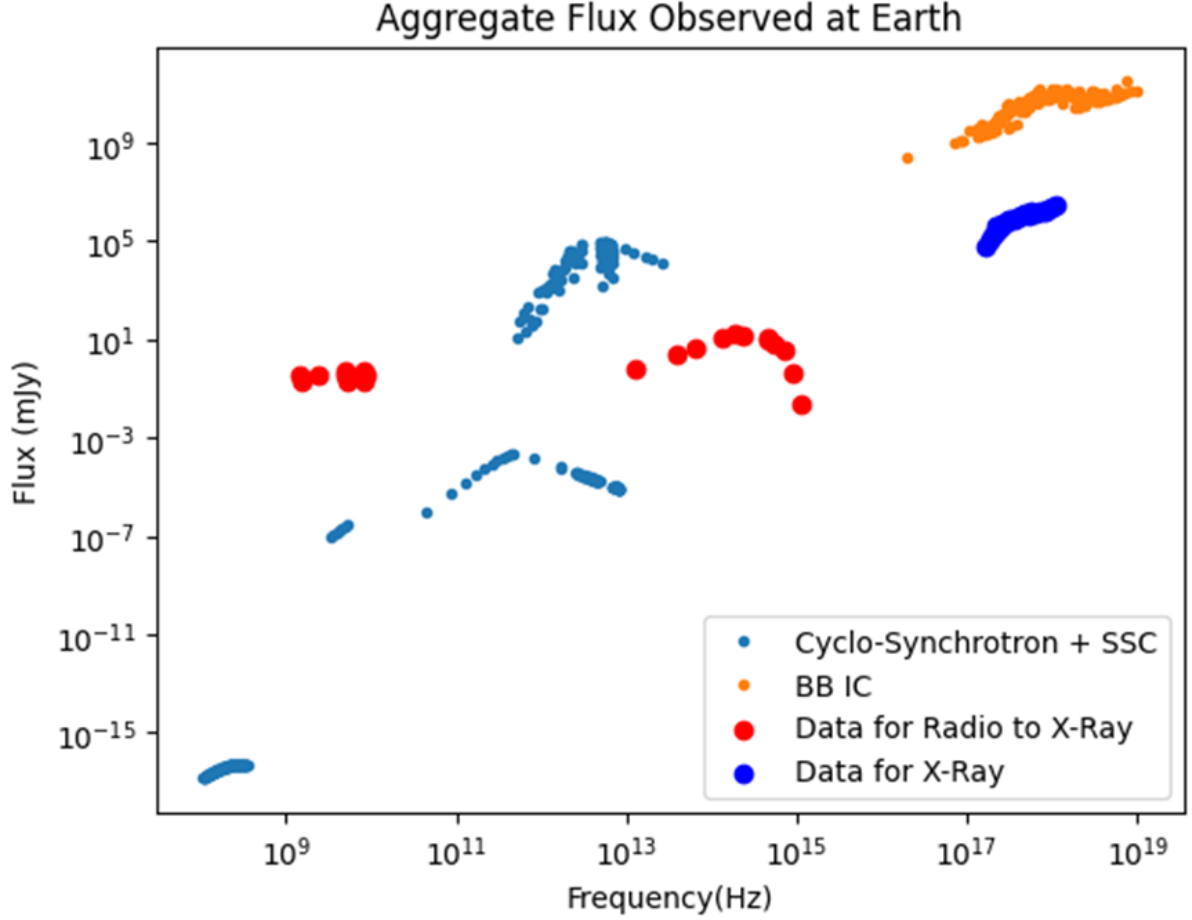


Figure 4: Aggregate flux spectrum observed at Earth, along with data points for radio and X-ray frequencies. There is overlap in the cyclosynchrotron and SSC emissions, which has been summed up. However, a spline or similar fit would be needed to get a meaningful plot.

Using $L_j = 10^{35}$, $R = 10 r_g$, $v = c/2$ (where $r_g = 10^6$, $c = 3 \times 10^{10}$), we obtain $B \sim 10^6$ G

This is very unphysical and large compared to the observed value, indicating that the source is not in equipartition configuration. This is probably a reason for the rightward shift of the synchrotron peak from expected value, as the calculation of emissivity, absorption, etc. assume an equipartition configuration. Also, the electron number density obtained from equipartition (10^{15} cm^{-3}) is used in computing the cyclotron spectrum.

Plasma beta for V404 Cygni in the hard state

$\beta_{Pl} = U_e/U_B \sim U_{tot}/U_B \sim 10^7$, where the magnetic field energy density has been calculated using the observed value of 33G (hence is very small compared to U_e)

3. Difference in order of magnitude between seed photons and scattered photons: For inverse Compton scattering from the accretion disk (blackbody) off the coronal electrons, we see a peak at around 10^{11} mJy at Earth. The input photon field (Planck function for temperature 10^7 K has a peak at around 10^4 in CGS units at the disk surface, which translates to about 1 mJy at Earth. Therefore, inverse Compton causes an upscattering by 10-11 orders of magnitude, which would imply a γ^2 of 10^{10} since it is basically the Lorentz factor that determines the order of upscattering. This gives a Lorentz factor of about 10^5 , which is quite different from the maximum of 100 that we have assumed.

Comparing with data however, the X-ray data has a peak at 10^4 mJy, suggesting a γ^2 of 10^4 , which agrees with our Lorentz factor! This means that we are obtaining an overestimation of photons from our Monte Carlo code. A similar overestimation is also seen in the case of SSC. According to me, the overestimation for blackbody IC is because of the following reasons:

a. We are assuming the corona to be a flat slab over the accretion disk, i.e. we are not taking the disk and

corona sizes and angles into account.

b. We are assuming a constant optical depth of 1.

c. We are ignoring any interstellar absorption.

d. We are assuming isotropy in the corona and constant disk and coronal temperatures. Furthermore, our coronal and disk radii may also be overestimated, leading to a larger photon count than there actually is. For the SSC, there are some other reasons that come into play:

a. For the Monte Carlo code, we assume the electrons to have a Maxwell Juttner distribution, while the emissivity and absorption for synchrotron self absorption assume a power law distribution. This is not a valid approximation for very relativistic electrons, as the Maxwell-Juttner provides a much lower value of electron density at higher lorentz factors as seen in fig 5. Therefore, we are obtaining an overestimation of photons from synchrotron self absorption, leading to a larger compton flux.

4. Compton spectrum cutoff at high frequencies:

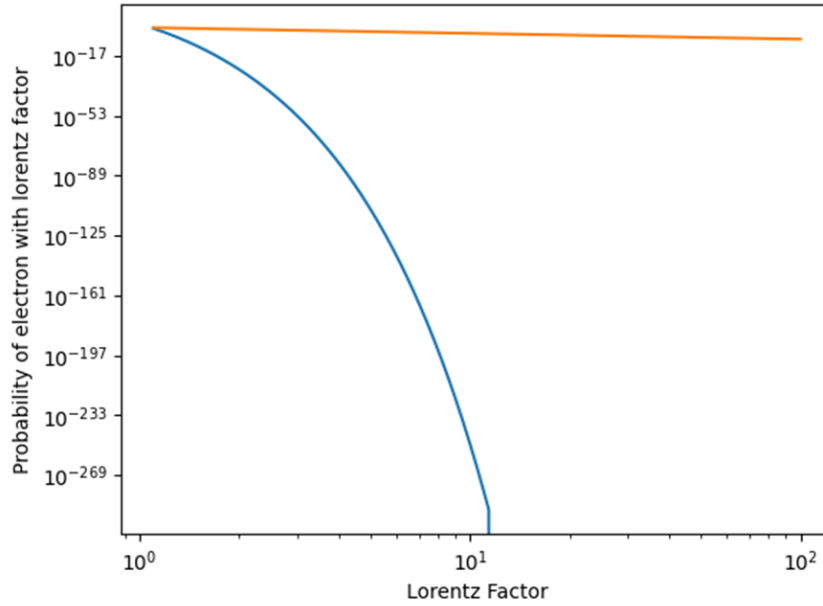


Figure 5: Electron distribution with respect to lorentz factor for a power law of 3.5 (orange) and a Maxwell Juttner distribution (blue).

We observe a cutoff in inverse compton scattering after a certain frequency for both SSC and blackbody inverse compton. This is essentially limited by the maximum energy of an electron. For a single scatter, the change in wavelength of a photon is given by:

$\lambda' - \lambda = \frac{h}{mc(1 - \cos x)}$ where m is the mass of an electron and x is the incident angle between the photon and the electron.

From this, we can find the maximum change in wavelength to be in the order 10^{-10} since h and m are of the order 10^{-27} and c is of the order 10^{10} in CGS units.

From this, for an accretion disk of temperature $10^7 K$, or a Wien's law peak at $10^{17} Hz$, we can observe a change in frequency of upto 3 orders of magnitude, i.e. the maximum frequency of scattered photons is $10^{20} Hz$. This matches with that observed from the model. We can replicate the same for the SSC as well.

5. Other Parameters:

a. In the model, we have assumed the black hole to be accreting at a rate corresponding to $10^{-4} L_{edd}$. This yields a luminosity of $10^{35} \text{ erg s}^{-1}$, which corresponds to a mass accretion rate of 10^{14} g/s or $10^{-12} M_{\odot} \text{ yr}^{-1}$. This is within the maximum limit of $10^{-10} M_{\odot} \text{ yr}^{-1}$ given by [Bartolomeo Koninckx, L. et al. \(2023\)](#).

b. Compton Y parameter: The Compton Y parameter for black body inverse Compton from our code is around 1.2, which is very similar to that given by [Motta et al. \(2017\)](#). The SSC Compton Y parameter is an order higher, which is mainly due to the higher optical depth. Varying the optical depth with frequency and other parameters would likely improve this (and also improve the overall shape and frequency range

of SSC).

4 Conclusion

To summarize, we have modelled the hard state of V404 Cygni assuming a corona and disk configuration. We have accounted for emissions due to cyclotron and synchrotron processes as well as inverse Compton scattering. We have however not modelled reflection spectra (time lags due to light from corona reflecting off the disk), or the blackbody emission from the disk itself. These would be present in the high X-ray and high optical to high UV range respectively. We have also made a lot of assumptions which have been discussed above. Some of these can be fixed with more rigorous models, like writing a more detailed monte carlo procedure that uses Klein Nishina instead of Thomson scattering, accounting for the angle between the disk and corona, varying optical depth with frequency for inverse Compton rather than keeping it constant, etc. More observations could also help constrain parameters, as currently X-ray data is from outbursts and radio is from quiescent state.

References

- Bartolomeo Koninckx, L. De Vito, M. A. Benvenuto, O. G. 2023, *A&A*, 674, A97
- Bernardini F., Russell D. M., Kolojonen K. I. I., Stella L., Hynes R. I., Corbel S., 2016, *The Astrophysical Journal*, 826, 149
- Dallilar Y., et al., 2017, *Science*, 358, 1299
- JAMES B. DOVE JÖRN WILMS M. M. A. M. C. B., 1997, *The Astrophysical Journal*, 487, 759
- Khargharia J., Froning C. S., Robinson E. L., 2010, *The Astrophysical Journal*, 716, 1105
- Koljonen, K. I. I. Tomsick, J. A. 2020, *A&A*, 639, A13
- Lucchini M., et al., 2022, *Monthly Notices of the Royal Astronomical Society*, 517, 5853
- Motta S. E., Kajava J. J. E., Sánchez-Fernández C., Giustini M., Kuulkers E., 2017, *Monthly Notices of the Royal Astronomical Society*, 468, 981
- 1985, SYNCHROTRON RADIATION. John Wiley Sons, Ltd, pp 167–194
(<https://onlinelibrary.wiley.com/doi/pdf/10.1002/9783527618170.ch6>),
[doi:https://doi.org/10.1002/9783527618170.ch6](https://doi.org/10.1002/9783527618170.ch6), <https://onlinelibrary.wiley.com/doi/abs/10.1002/9783527618170.ch6>
- Sebastian Heinz 2023, Monte-Carlo Inverse Compton Tutorial